On the Importance of a Geostationary View for Tropical Cloud Feedback

Yoon-Kyoung Lee[1] ![ORCID], **Yong-Sang Choi[1]** ![ORCID], **Jiwon Hwang[2]** ![ORCID], **Xiaoming Hu[3]** ![ORCID], and **Song Yang[3]** ![ORCID]

[1]Center for Climate/Environmental Change Prediction Research, Ewha Womans University, Seoul, Korea, [2]Korea Institute of Corporate Governance and Sustainability, Seoul, Korea, [3]School of Atmospheric Sciences, Sun Yat-sen University, and Southern Marine Science and Engineering Guangdong Laboratory (Zhuhai), Zhuhai, China

Abstract This study shows that geostationary satellites are critical to estimate the accurate cloud feedback strength over the tropical western Pacific (TWP). Cloud feedback strength was calculated by the simultaneous relation between cloud cover and sea surface temperature (SST) over the TWP [120°E–170°E, 20°S–20°N]. During 2011–2018, the cloud cover was obtained by geostationary earth orbit satellite (GEO) and low-level earth orbit satellite (LEO) (A^{GEO}, A^{LEO}), and the NOAA's all-sky SST (T_o) was weighted with the clear-sky fraction observed by GEO and LEO (T_w^{GEO}; T_w^{LEO}). The linear regression coefficients between clouds and SST are very different: $-7.93\%K^{-1}$ (A^{GEO}/T_w^{GEO}), $-6.94\%K^{-1}$ (A^{LEO}/T_w^{GEO}), $-1.35\%K^{-1}$ (A^{GEO}/T_w^{LEO}), -0.69 K^{-1} (A^{LEO}/T_w^{LEO}), $-0.02\ \%K^{-1}$ (A^{GEO}/T_o), and $-0.50\ \%K^{-1}$ (A^{LEO}/T_o). Among these, only the T_w^{GEO} values provided a valid cloud feedback signal. This is because GEO's field of view is large enough to simultaneously capture cloud cover over the entire TWP.

Plain Language Summary Geostationary satellites are essential for accurately estimating cloud feedback strength over the tropical western Pacific (TWP). Cloud feedback strength is the change in cloudiness that results from a change in sea surface temperature (SST). When using data from both geostationary and low-earth orbit satellites, the resulting cloud feedback signals are very different. This is because geostationary satellites have a large enough field of view to capture cloud cover over the entire TWP, while low-earth orbit satellites do not. Therefore, geostationary satellites are the only reliable source of data for estimating cloud feedback strength over the TWP. This is important because cloud feedback is a major uncertainty in climate models.

1. Introduction

Clouds play an important role in regulating the radiation budget in the climate system, reflecting incoming shortwave (SW) radiation and trapping outgoing longwave (LW) radiation. The effective radiation control effect of clouds depends on their area, height, and thickness. The morphology of the clouds is determined by various factors such as ground temperature, sea surface temperature (SST), water vapor in the atmosphere, stability, and wind patterns. Among those climate variables, the SST is the measure of cloud feedback as a force and response of cloud changes.

In general, when SST rises, convective activity increases, which then promotes cloud formation. In particular, convective clouds over the TWP are known to be sensitive to local SST (between 26 and 30°C) (Fu et al., 1992; Gill & Rasmusson, 1983; Tompkins, 2001; Zhang, 1993). Clouds found in the moist region of the TWP in the upper troposphere are mainly cirrus clouds. As these clouds cover a vast area, they can effectively block LW radiation to space (Kiehl, 1994) and determined SST. Therefore, the expansion and contraction of these clouds can dramatically affect the climate system over the TWP (Gao et al., 2009).

The key challenges in measuring cloud feedback strength are the interactions between clouds and SST are not clearly identified since both cloud and SST are individually affected by a variety of factors. A number of previous studies have investigated the relationship between TWP clouds and SST using observational data (Albrecht, 1981; Betts & Ridgway, 1989; Cesana et al., 2019; Cho et al., 2012; Choi et al., 2017; Gao et al., 2009; Horváth & Soden, 2008; Norris & Leory, 1994; Oreopoulos & Davies, 1993; Ramanathan & Collins, 1991; Schiro et al., 2022; Zhang, 1993). Nevertheless, a little is known on cloud feedback strength due to widely varied cloud-SST relationships, ranging from negative to positive. The reason behind the inconsistent results on the cloud-SST relationship so far is very low correlation based on a lack of distinction of their causality in the

dynamic system. A simple analysis of the two-year observational data showed that the cloud-SST relationship was statistically insignificant (Choi et al., 2005). The correlation coefficient between clouds and SST change within the TWP is usually very low ($r = -0.1$), and the regression slope $-6\%/K$ from Cho et al. (2012). This low correlation is because the formation and development of clouds are determined by various factors other than SST, the correlation between clouds and SST may be reduced.

Satellite data plays a vital role in addressing these challenges. Recent active satellite sensors that can resolve vertical profiles of clouds have shown that anvil cirrus clouds tend to decrease with increasing SST (Igel et al., 2014). When SST increases, TWP clouds (mainly cirrus) decrease at a rate of $-22\%/°C$ (Lindzen et al., 2001) and $-14.4\%/K$ (Cho et al., 2012) in geostationary satellite observations. The cloud reduction may be due to the thermodynamic effects of the atmosphere, including increased water vapor (Bony et al., 2016; Bretherton, 2015; Sherwood et al., 2020). In contrast, other studies have shown an increase in cloud amount (and reduction in outgoing LW radiation) with increasing SST (Albrecht, 1981), implying positive or near-zero cloud feedback over the tropical convection region. Therefore, considerable uncertainties remain surrounding cloud feedback, as suggested by several previous studies (Schiro et al., 2022; Sherwood et al., 2014, 2020; Zelinka et al., 2022). In current climate models (CMIP5 and CMIP6), tropical upper-level clouds tend to have negative feedback, while other types of clouds have positive feedback (Sherwood et al., 2020; Zelinka et al., 2022).

In this study, we compare data from geostationary earth orbit satellites (GEO) and low-level earth orbit satellites (LEO) to determine the effect of the observation period and range of satellite sensors. The difference in cloud feedback between the two satellite data sets has not previously been documented. The cloud response to SST changes occurs within minutes to hours, and a low-orbit satellite passing twice a day may not be able to capture the instantaneous reaction of these clouds. In addition, in the case of active satellite sensors such as CALIOP and CloudSat, the viewing swath (70–300 m for CALIOP, ~1.4 km for CloudSat) is very narrow, so they may not be able to observe large-scale areal responses of clouds. However, cloud data from GEO can capture fast cloud response to changes in SST (Lindzen et al., 2001). Additionally, GEO has the advantage of extracting clear-sky (cloudless) SST. This clear-sky SST can reduce noise caused by autonomous clouds, and would help to find better signals of cloud reactions to SST (Cho et al., 2012). We also examined the time lag relationship between the cloud and SST to further identify the causality and to estimate cloud feedback strengths with least uncertainty. Ultimately, this study attempts to understand the characteristics and limitations of cloud feedback estimates by comparing different orbits of GEO and LEO.

2. Data and Methods

The domain for this study is called the tropical western Pacific (TWP) region in several previous studies (Horváth & Soden, 2008; Lindzen et al., 2001; Ramanathan & Collins, 1991). Our analysis region (120°E–170°E, 20°S–20°N) is slightly different from those used in previous studies ((130°E–170°W, 20°S–20°N) in Cho et al. (2012) and (120°E–155°W, 30°S–30°N) in Lindzen et al. (2001) and Choi et al. (2017)) due to the limited field of view of GEO.

We used the cloud cover data from two types of satellites (geostationary orbit satellite vs. sun-synchronous orbit satellite) to compare the characteristics of each data set. The criteria for selecting GEO satellite data used in this study are noteworthy. First, both satellites should cover the TWP, although the orbits are different. The major difference is that GEO captures the entire TWP simultaneously, like a snapshot, and LEO provides observations twice daily. Second, at least 3-hourly cloud data (continuously observed from a single GEO for several years) should be available. Lastly, GEO data should cover LEO observation period. As we will use MODIS/Terra as LEO, the GEO data that meet those criteria are the cloud cover data set is obtained by the Korean National Meteorological Satellite Center's Communication, Ocean and Meteorological Satellite (COMS). The COMS, the first Korean geostationary meteorological satellite, was launched in June 2010. Their highest temporal resolution for the full-disk image is 3-hr. The 3-hourly data are available for the eight-years from 2011 to 2018. It is stationed at an altitude of 36,000 km above the Earth's equator and centered at a longitude of 128.15°E (moved slightly from 128.2°E after GEO-KOMPSAT-2A was launched). COMS has an imager and an ocean color sensor that are used for meteorological and oceanographical missions, respectively (Choi et al., 2007). The COMS meteorological mission is performed by the Meteorological Imager (MI) with one visible channel (0.67 μm) and four infrared channels (3.7, 6.7, 10.8, and 12.0 μm), with spatial resolutions of 1 km and 3–4 km, respectively (Choi et al., 2007; Kim & Ahn, 2014) (for more details about cloud detection, see Choi et al., 2007).

Table 1
Definition of Variables Used in This Study

	Variable/source	Reference
T_o	SST/OISST v2 from NOAA (no weighting)	
$T_w{}^{GEO}$	SST weighted by MI/COMS	Cho et al. (2012)
$T_w{}^{LEO}$	SST weighted by MODIS/Terra	
A^{GEO}	Cloud fraction of MI/COMS	
A^{LEO}	Cloud fraction of MODIS/Terra	

For comparison, an additional cloud-cover data set was sourced from the Moderate Resolution Imaging Spectroradiometer (MODIS) of the National Aeronautics and Space Administration (NASA) on the Terra platform (https://atmosphere-imager.gsfc.nasa.gov). Level 3 atmospheric data carries a spatial resolution of $1° \times 1°$. MODIS serves as a pivotal instrument on both the Terra (originally known as EOS AM-1) and Aqua (originally known as EOS PM-1) satellites. Terra's orbit around the Earth is timed so that it passes from north to south across the equator in the morning. The MODIS instrument has a 2,330 km viewing swath width and captures the entire Earth's surface every one to two days. The MODIS conducts observations once daily, while the COMS provides hourly surveillance. Hereafter, we denote the MI/COMS within the geostationary Earth orbit as GEO, and the MODIS/Terra within the low-level Earth orbit as LEO.

This study can be affected by the bias of satellite data. Satellite data have systematic errors, such as inaccuracies in equipment or measurement methods or errors in model background. Recent validation results of GEO's cloud data by referring to LEO show that the mean bias was −3.83% to −3.57% and the root mean square error was 21.68%–22.48% in global scale. However, GEO and LEO are highly correlated (the correlation coefficient is 0.89 for daily data and 0.88 for monthly data). In addition, the GEO cloud detection algorithm did not perform bias correction for the daily sun glint area. Therefore, the sun glint areas were not excluded in this study.

For the analysis, 3-hourly and 4 km × 4 km cloud amount data set from COMS Level 2 Cloud Products is converted to the gridded data with a resolution of $0.5° \times 0.5°$. Then, the 3-hourly grid data is aggregated into daily data by averaging eight sets of 3-hourly grid data corresponding to the following UTC times: 02:15, 05:15, 08:15, 11:15, 14:15, 17:15, 20:15, and 23:15. Similarly, monthly COMS cloud cover data is processed by averaging these daily cloud cover data sets. MODIS monthly and daily cloud cover data are obtained from Level 3 MOD08_M3 version 6 and MOD08_D3 version 6.

The SST data is from the National Oceanic and Atmospheric Administration (NOAA) OISSTv2 (the optimal interpolated SST version 2), which uses microwave satellite measurements from the Advanced Microwave Scanning Radiometer (AMSR) and infrared satellite measurements from the Advanced Very High Resolution Radiometer (AVHRR) (Reynolds et al., 2007). This data can include SSTs that have already changed due to cloud effects. The horizontal resolution is $1° \times 1°$ global grid (180×360) for the monthly timescale, and $0.25° \times 0.25°$ global grid (1440×720) for the daily timescale. For a shorter timescale, we additionally used 3-hourly SST data from COMS Level 2 data. COMS SST represents only clear-sky SST with no cloud effect.

Clear-sky SST is required for cloud feedback analysis due to the potential influence of cloud cover on SST (Cho et al., 2012). The work of Cho et al. (2012) disentangles SST variations originating from cloud variations from those arising from cloud cover changes. We apply this method to minimize the noise effects and consider solely the cloud response prompted by SST change (excluding SST response to cloud variation). To distinguish the difference from the noise effect, two terms for SST are used in this study (in Table 1 and Figure 1): all-sky SST (T_o) and clear–sky SST (T_w), where the subscripts o and w indicate observation and cloud amount weightings, respectively. T_o indicates the all-sky SSTs (non–weighted SSTs), while $T_w{}^{GEO}$ and $T_w{}^{LEO}$ denote the clear-sky SSTs weighted by cloud amount of the GEO and LEO platforms, respectively (see the equation in Figure 1). T_w is calculated at each grid cell by applying a weight to the clear-sky value using cloud amount data from GEO and LEO (Figure 1). The time series of cloud amount and SST anomalies are obtained as area-averaged values over the TWP [120°E–170°E, 20°S–20°N]. In this study, all variables are anomaly data, calculated by subtracting climatological mean from monthly (or daily) mean. A^{GEO} and A^{LEO} indicate cloud amounts observed by MI/COMS and MODIS/Terra, respectively (as specified in Table 1).

3. Comparison of Cloud Feedback to SST Change in GEO and LEO

Prior to comparing cloud feedback to SST change within GEO and LEO contexts, we first examined the variation of T_o and T_w (Figure 2). To eliminate the cloud-induced influence on SST (as elucidated in Section 2), we use the clear-sky SST by employing cloud amount data at each grid cell. Clear-sky SST is used instead of all-sky SST to remove noise, aligning with the insights of Cho et al. (2012). The time series of the SST anomalies, both T_o (black line) and T_w (red line for GEO and blue line for LEO) show similar variations in the monthly timescale (Figure 2a). Both curves show a temperature rise in 2016. However, when shifting the focus to the daily timescale,
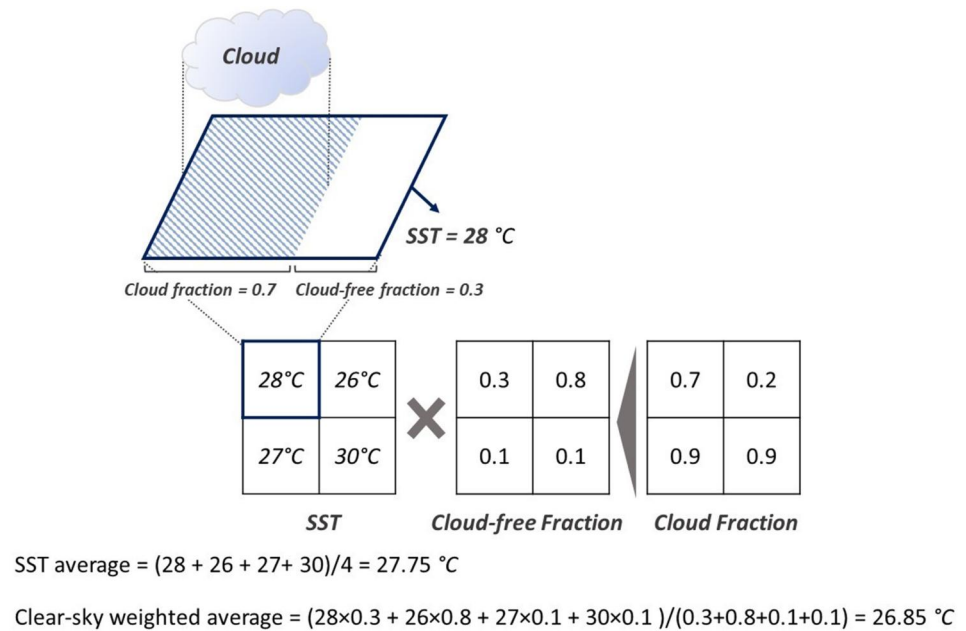
Figure 1. An illustration of calculation in cloud-free SST from SST and cloud fraction data.

distinct patterns emerge between all-sky and clear-sky conditions (Figure 2b). There are larger fluctuations in clear-sky conditions than in all-sky conditions. Showing similar patterns on all monthly scales means capturing low-frequency patterns well. Conversely, the divergence between the two conditions in high–frequency patterns imply variability related to cloud amount.

The relationship between cloud amount (A) and SST (T) was evaluated on monthly (not shown) and daily timescales. It is necessary to investigate the dynamic lead-lag relationship between these two variables.
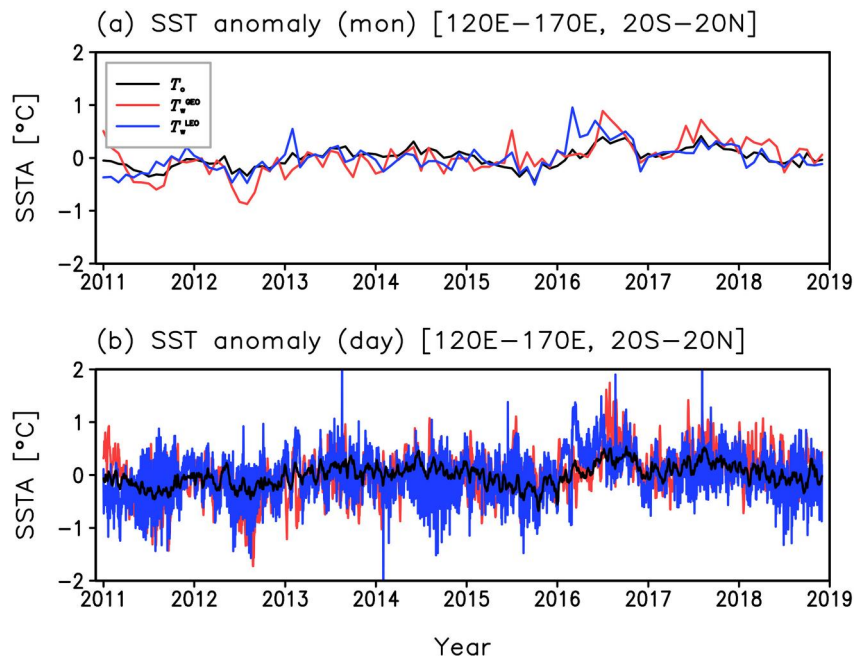
Figure 2. Time series of (a) monthly and (b) daily SST anomaly. The black line indicates the original SST, and the red (blue) line indicates SST weighted with GEO (LEO) cloud cover.
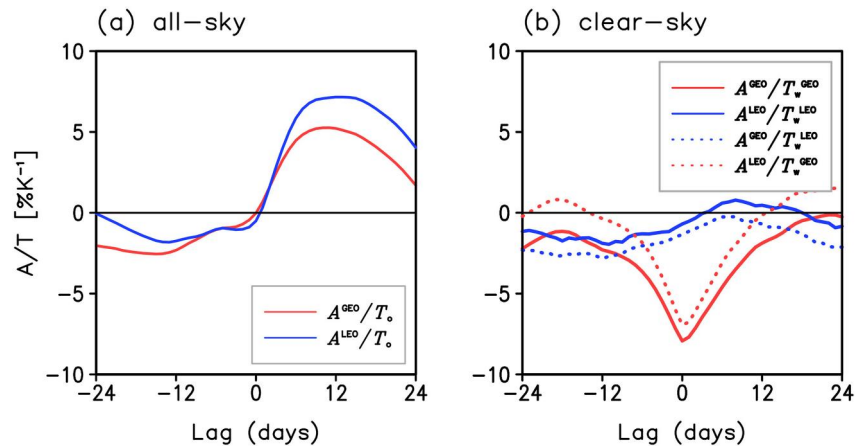
Figure 3. Lagged regression slopes between A and T in a daily timescale for (a) all-sky and (b) clear-sky condition. A and T are the anomalies against the area-averaged value over the TWP. Red (blue) line indicates the regression slope between A^{GEO} (A^{LEO}) and T_o in (a). In (b), red (blue) solid line indicates the regression slope between A^{GEO} and T_w^{GEO} (between A^{LEO} and T_w^{LEO}), and blue (red) dotted line indicates the regression slope between A^{GEO} and T_w^{LEO} (between A^{LEO} and T_w^{GEO}).

Figure 3 shows the lagged regression slopes between A and T in a daily timescale, where a negative lag indicates A leading T, and a positive lag implies T leading A. Notably, at the zero-lag point, the relationship tends to be statistically insignificant in both the monthly timescale and all-sky condition in the daily timescale. The regression slopes are $-0.02\%K^{-1}$ for A^{GEO}/T_o (red solid line), and $-0.50\%K^{-1}$ for A^{LEO}/T_o (blue solid line) at the daily timescale (Figure 3a). Here, we tried to use the clear-sky SST weighted by cloud cover to discern discrepancies in cloud detection across various data sets (Figure 3b). A^{GEO}/T_w^{GEO} exhibited a significant negative correlation with its minimum peak of regressed slope at zero lag. The corresponding regression slope for A^{GEO}/T_w^{GEO} is $-7.93\%K^{-1}$ (red solid line). In this case, the sharp V-shaped pattern with a peak at zero lag confirms the validity of the slope. It is worth noting that convex (or opposite) shape in the lead–lag relationship gives the signal of the cloud's response to SST change from the regression slope at "zero" lag (Frankignoul et al., 1998; Lindzen & Choi, 2011). This shape does not appear when the non-weighted SST (T_o) is employed. A^{GEO}/T_o (A^{LEO}/T_o) is negative at negative lag, transitioning into positive values at positive lags. This result implies that increased A cools the SST owing to the cloud-induced effect (Cho et al., 2012). The regressed slopes, A^{LEO}/T_w^{LEO} ($-0.69\%K^{-1}$, blue solid line) and A^{GEO}/T_w^{LEO} ($-1.35\%K^{-1}$, blue dotted line) show similar shapes to results in Figure 3a, even using the clear-sky SST. The relationships demonstrate almost negligible correlation at zero lag. However, when T_w^{GEO} is used, the regressed value becomes $-6.94\%K^{-1}$ for A^{LEO}/T_w^{GEO} (red dotted line). A^{GEO}/T_w^{GEO} and A^{LEO}/T_w^{GEO} have maximum negative correlation at zero-time lag. This strong negative relation at the daily timescale is absent when T_o or longer timescale data (e.g., monthly timescale data) is employed. For the TWP region, it is well established that the lifetime of cloud processes linked to cumulonimbus ranges from hours to days. Consequently, it is reasoned that such a relationship does not appear in the monthly timescale results. The negative correlation shows that the cloud cover decreases with the increase in the SST, which aligns with findings from previous studies.

The spatial pattern of the regressed A/T ratios for the daily timescale is shown in Figure 4. Cloud amount in GEO corresponds to a negative correlation with SST over the majority of the analysis area (Figure 4a). The regressed maps A^{LEO}/T_w^{LEO} and A^{GEO}/T_w^{GEO} show a positive correlation in the western side but a negative correlation in the eastern side of the analysis area. As in Figure 3, the regressed map A^{LEO}/T_w^{GEO} shows a negative correlation when T_w^{GEO} is employed. This difference comes from the broader field-of-view of GEO that can cover the entire TWP, as opposed to the limited scope of LEO.

We also calculated the regressed slope A^{GEO}/T_w^{GEO} with 3-hourly data (not shown). The 3-hourly SST data is only available in GEO and observed under the clear-sky conditions in GEO. The regressed map between A^{GEO} and T_w^{GEO} at the 3–hourly timescale was analyzed in the same way as in other timescale data. Both analyses yield the same results as those observed at the daily timescale. This result indicates that the shorter timescales (3-hourly to daily) can resolve the relationship between cloud amount and SST than a monthly timescale.
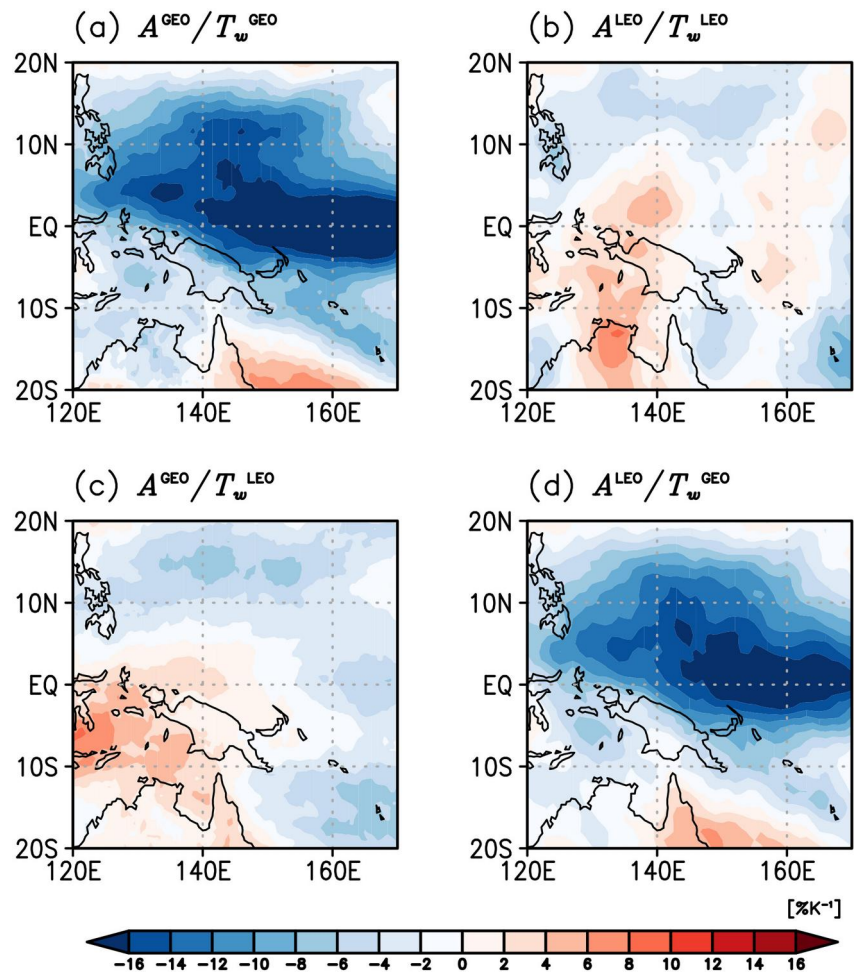
Figure 4. Regressed map of (a) A^{GEO} onto T_w^{GEO}, (b) A^{LEO} onto T_w^{LEO}, (c) A^{GEO} onto T_w^{LEO}, and (d) A^{LEO} onto T_w^{GEO} over the TWP in a daily timescale.

Additionally, we confirmed that these negative correlations were not dependent on averaging the entire TWP region. The results of negative correlations were similar to the results calculated by dividing the analysis area into each segment of about 10° of latitude and 10° of longitude. Specifically, strong negative correlations were identified in the Northern Hemisphere (0°–20°N), but weak positive and negative correlations occurred around the Southern Hemisphere, the boundary of the analysis region shown in the entire area average result (not shown). The relationship was investigated by adjusting the analysis area by 20° in the latitude/longitude direction, and the negative correlation was similar to that calculated by dividing it by about 10° latitude and about 10° longitude, respectively. Same as before, there was a strong negative correlation in the Northern Hemisphere, with weak positive correlations and negative correlations around the Southern Hemisphere, which is shown in the overall regional mean results (not shown). These weak correlations over the Southern Hemisphere are due to the location of the maritime continent.

4. Summary

In this study, we examined the cloud feedback over the TWP by using two types of satellite data (GEO and LEO) with different timescales (from hourly to monthly). We analyzed the cloud variation against clear-sky SST to reduce the noise in the original SST that can be affected by cloud cover. The regressed slope of cloud cover and SST (A/T) varies depending on the type of data (weighted or non–weighted SST in hourly-to-monthly time-scales). The maximum negative peak at zero-time lag only appears in daily timescale data with clear-sky SST from geostationary satellites (T_w^{GEO}). The negative correlations between A and T show that cloud amount

decreases as SST increases. The negative signals are distributed over the entire domain when using T_w^{GEO} in daily timescale data. The importance of our result is that the significant relationship only appears in the daily data that come from data set when using the geostationary satellite data. We also found a strong negative relation using the 3-hr data. It may not be resolved in data sets with longer than a daily timescale, or in data from satellites with non-sun-synchronous orbits. For the cloud feedback system, the data timescale is very important to resolve the relation between cloud and SST change. As mentioned earlier, this is because the life time of cloud processes is from hours to days.

The different results between T_w^{GEO} and T_w^{LEO} can also be considered due to the difference in observed spatial coverage. Whereas the GEO satellite continues to observe the same area at once, the LEO satellite orbits twice daily, and the data obtained by LEO through this process do not completely capture the analysis area at the same time. In the analysis area in this study, when using SST weighted by LEO cloud cover (Figures 4b and 4c), both the negative and positive signals appear. The distance at which the opposite sign appears is similar to the viewing swath of the LEO (2,330 km). The LEO observations (cloud fraction data from LEO; MODIS) shows that high-level clouds have positive correlation over equatorial Indian Ocean and negative correlation over North Bay of Bengal (Chaudhari et al., 2016). The results are similar to Figures 4b and 4c. Given this result, it is also possible to think about the difference in observe-time that appears in observation. Therefore, it is more effective to use high temporal resolution data from geostationary satellites to reduce noise of SST in the TWP. Reducing noise is eventually important for reducing uncertainty in observational estimates of cloud feedback.

Cloud feedback is one of the factors that greatly affect climate change. Yet, the current simulations of cloud cover in climate models are very uncertain, and the differences in cloud feedback among the climate models remain large. Further studies need to investigate physical mechanism behind the cloud feedback strength found in our study.

Data Availability Statement

MI/COMS cloud data are http://datasvc.nmsc.kma.go.kr/datasvc/html/data/listData.do?lang=ko (registration and request is required). The MODIS/Terra cloud products are available from the Atmosphere Archive and Distribution System (LAADS) Distributed Active Archive Center (DAAC): https://ladsweb.modaps.eosdis.nasa.gov/archive/allData/61/MOD08_M3 for monthly and https://ladsweb.modaps.eosdis.nasa.gov/archive/allData/61/MOD08_D3 for daily. NOAA OISSTv2 data can be obtained from the website at https://psl.noaa.gov/data/gridded/data.noaa.oisst.v2.highres.html.

References

Albrecht, B. A. (1981). Parameterization of trade-cumulus cloud amounts. *Journal of the Atmospheric Sciences*, *38*(1), 97–105. https://doi.org/10.1175/1520-0469(1981)038<0097:potcca>2.0.co;2

Betts, A. K., & Ridgway, W. (1989). Climatic equilibrium of the atmospheric convective boundary layer over a tropical ocean. *Journal of the Atmospheric Sciences*, *46*(17), 2621–2641. https://doi.org/10.1175/1520-0469(1989)046<2621:ceotac>2.0.co;2

Bony, S., Stevens, B., Coppin, D., Becker, T., Reed, K. A., Voigt, A., & Medeiros, B. (2016). Thermodynamic control of anvil cloud amount. *Proceedings of the National Academy of Sciences*, *113*(32), 8927–8932. https://doi.org/10.1073/pnas.1601472113

Bretherton, C. S. (2015). Insights into low-latitude cloud feedbacks from high-resolution models. *Philosophical Transactions of the Royal Society A*, *373*(2054), 20140415. https://doi.org/10.1098/rsta.2014.0415

Cesana, G., Del Genio, A. D., Ackerman, A. S., Kelley, M., Elsaesser, G., Fridlind, A. M., et al. (2019). Evaluating models' response of tropical low clouds to SST forcings using CALIPSO observations. *Atmospheric Chemistry and Physics*, *19*(5), 2813–2832. https://doi.org/10.5194/acp-19-2813-2019

Chaudhari, H. S., Pokhrel, S., Kulkarni, A., Hazra, A., & Saha, S. K. (2016). Clouds-SST relationship and interannual variability modes of Indian summer monsoon in the context of clouds and SSTs: Observational and modelling aspects. *International Journal of Climatology*, *36*(15), 4723–4740. https://doi.org/10.1002/joc.4664

Cho, H., Ho, C.-H., & Choi, Y.-S. (2012). The observed variation in cloud induced longwave radiation in response to sea surface temperature over the Pacific warm pool from MTSAT-1R imagery. *Geophysical Research Letters*, *39*(18), L18802. https://doi.org/10.1029/2012GL052700

Choi, Y.-S., Ho, C.-H., Ahn, M.-H., & Kim, Y.-M. (2007). An exploratory study of cloud remote sensing capabilities of the Communication, Ocean and Meteorological Satellite (COMS) imagery. *International Journal of Remote Sensing*, *28*(21), 4715–4732. https://doi.org/10.1080/01431160701264235

Choi, Y.-S., Ho, C.-H., & Sui, C.-H. (2005). Different optical properties of high cloud in GMS and MODIS observations. *Geophysical Research Letters*, *32*(23), L23823. https://doi.org/10.1029/2005GL024616

Choi, Y.-S., Kim, W., Yeh, S.-W., Masunaga, H., Kwon, M.-J., Jo, H.-S., & Huang, L. (2017). Revisiting the Iris effect of tropical cirrus clouds with TRMM and A-train satellite data. *Journal of Geophysical Research: Atmospheres*, *122*(11), 5917–5931. https://doi.org/10.1002/2016JD025827

Frankignoul, C., Czaja, A., & L'Heveder, B. (1998). Air–sea feedback in the north Atlantic and surface boundary conditions for ocean models. *Journal of Climate*, *11*(9), 2310–2324. https://doi.org/10.1175/1520-0442(1998)011<2310:ASFITN>2.0.CO;2

Fu, R., Del Genio, A. D., Rossow, W. B., & Liu, W. T. (1992). Cirrus cloud thermostat for tropical sea surface temperatures tested using satellite data. *Nature*, *358*(6385), 394–397. https://doi.org/10.1038/358394a0

Gao, S., Cui, X., & Li, X. (2009). A modeling study of relation between cloud amount and SST over Western Tropical Pacific cloudy regions during TOGA COARE. *Progress in Natural Science*, *19*(2), 187–193. https://doi.org/10.1016/j.pnsc.2008.07.006

Gill, A., & Rasmusson, E. (1983). The 1982–83 climate anomaly in the equatorial Pacific. *Nature*, *306*(5940), 229–234. https://doi.org/10.1038/306229a0

Horváth, Á., & Soden, B. J. (2008). Lagrangian diagnostics of tropical deep convection and its effect upon upper-tropospheric humidity. *Journal of Climate*, *21*(5), 1013–1028. https://doi.org/10.1175/2007JCLI1786.1

Igel, M. R., Drager, A. J., & van den Heever, S. C. (2014). A CloudSat cloud object partitioning technique and assessment and integration of deep convective anvil sensitivities to sea surface temperature. *Journal of Geophysical Research: Atmospheres*, *119*(17), 10515–10535. https://doi.org/10.1002/2014JD021717

Kiehl, J. (1994). On the observed near cancellation between longwave and shortwave cloud forcing in tropical regions. *Journal of Climate*, *7*(4), 559–565. https://doi.org/10.1175/1520-0442(1994)007<0559:otoncb>2.0.co;2

Kim, D. H., & Ahn, M. H. (2014). Introduction of the in-orbit test and its performance for the first meteorological imager of the communication, Ocean, and Meteorological Satellite. *Atmospheric Measurement Techniques*, *7*(8), 2471–2485. https://doi.org/10.5194/amt-7-2471-2014

Lindzen, R. S., & Choi, Y.-S. (2011). On the observational determination of climate sensitivity and its implications. *Asia-Pacific Journal of Atmospheric Sciences*, *47*(4), 377–390. https://doi.org/10.1007/s13143-011-0023-x

Lindzen, R. S., Chou, M.-D., & Hou, A. Y. (2001). Does the Earth have an adaptive infrared iris? *Bulletin of the American Meteorological Society*, *82*(3), 417–432. https://doi.org/10.1175/1520-0477(2001)082<0417:DTEHAA>2.3.CO;2

Norris, J. R., & Leory, C. B. (1994). Interannual variability in stratiform cloudiness and sea surface temperature. *Journal of Climate*, *7*(12), 1915–1925. https://doi.org/10.1175/1520-0442(1994)007<1915:IVISCA>2.0.CO;2

Oreopoulos, L., & Davies, R. (1993). Statistical dependence of albedo and cloud cover on sea surface temperature for two tropical marine stratocumulus regions. *Journal of Climate*, *6*(12), 2434–2447. https://doi.org/10.1175/1520-0442(1993)006<2434:SDOAAC>2.0.CO;2

Ramanathan, V., & Collins, W. (1991). Thermodynamic regulation of ocean warming by cirrus clouds deduced from observations of the 1987 El Niño. *Nature*, *351*(6321), 27–32. https://doi.org/10.1038/351027a0

Reynolds, R. W., Smith, T. M., Liu, C., Chelton, D. B., Casey, K. S., & Schlax, M. G. (2007). Daily high-resolution-blended analyses for sea surface temperature. *Journal of Climate*, *20*(22), 5473–5496. https://doi.org/10.1175/2007JCLI1824.1

Schiro, K. A., Su, H., Ahmed, F., Dai, N., Singer, C. E., Gentine, P., et al. (2022). Model spread in tropical low cloud feedback tied to overturning circulation response to warming. *Nature Communications*, *13*(1), 7119. https://doi.org/10.1038/s41467-022-34787-4

Sherwood, S., Bony, S., & Dufresne, J. L. (2014). Spread in model climate sensitivity traced to atmospheric convective mixing. *Nature*, *505*(7481), 37–42. https://doi.org/10.1038/nature12829

Sherwood, S. C., Webb, M. J., Annan, J. D., Armour, K. C., Forster, P. M., Hargreaves, J. C., et al. (2020). An assessment of Earth's climate sensitivity using multiple lines of evidence. *Reviews of Geophysics*, *58*(4), e2019RG000678. https://doi.org/10.1029/2019RG000678

Tompkins, A. M. (2001). On the relationship between tropical convection and sea surface temperature. *Journal of Climate*, *14*(5), 633–637. https://doi.org/10.1175/1520-0442(2001)014<0633:OTRBTC>2.0.CO;2

Zelinka, M. D., Klein, S. A., Qin, Y., & Myers, T. A. (2022). Evaluating climate models' cloud feedbacks against expert judgment. *Journal of Geophysical Research: Atmospheres*, *127*(2), e2021JD035198. https://doi.org/10.1029/2021JD035198

Zhang, C. (1993). Large-scale variability of atmospheric deep convection in relation to sea surface temperature in the tropics. *Journal of Climate*, *6*(10), 1898–1913. https://doi.org/10.1175/1520-0442(1993)006<1898:LSVOAD>2.0.CO;2